Journal of Saudi Chemical Society (2017) **21**, 172–179

King Saud University

**Journal of Saudi Chemical Society**

www.ksu.edu.sa
www.sciencedirect.com

ORIGINAL ARTICLE

# Bio inspired synthesis of monodispersed silver nano particles using *Sapindus emarginatus* pericarp extract – Study of antibacterial efficacy

**G. Cynthia Jemima Swarnavalli [a,*], S. Dinakaran [b], N. Raman [c], R. Jegadeesh [d], Carol Pereira [e]**

[a] *Department of Chemistry, Women's Christian College, Chennai 600006, India*
[b] *School of Advanced Sciences, VIT University, Vellore 632014, India*
[c] *Department of Botany, University of Madras, Chennai 600025, India*
[d] *Mushroom Research Centre, University of Malaya, Kuala Lumpur 50603, Malaysia*
[e] *P.G. & Research Department of Adv. Zoology and Biotechnology, Loyola College, Chennai 600034, India*

Received 10 September 2014; revised 3 March 2015; accepted 8 March 2015
Available online 21 April 2015

**KEYWORDS**

Silver nanoparticles;
*Sapindus emarginatus* extract;
XRD;
TEM;
Antimicrobial activity

**Abstract** The synthesis of silver nanoparticles employing aqueous extract obtained from the dried pericarp of "*Sapindus emarginatus*" is reported. Transmission electron microscopy divulges that the silver nanoparticles are not agglomerated and are moderately mono dispersed. Size of the particle ranges from 5 to 20 nm with an average particle size of 10 nm. Ultraviolet–visible spectra recorded show typical surface plasmon resonance (SPR) at 400 nm. X-ray diffraction analysis reveals the crystalline nature of the synthesized silver nanoparticles with face-centred cubic (FCC) geometry. Silver nanoparticles thus obtained demonstrated remarkable antibacterial activity against *Bacillus subtilis*, *Staphylococcus aureus*, *Escherichia coli*, *Proteus mirabilis*, *Proteus vulgaris*, *Klebsiella pneumonia*, *Pseudomonas aeruginosa* and *Vibrio cholerae*. Freshly prepared samples and sample containing 6 nm silver nanoparticles in particular exhibited enhanced activity against gram positive bacteria. The minimal inhibitory concentration was found to be in the range of 150–250 μg/mL.


## 1. Introduction

Antimicrobial properties of silver especially silver nanoparticles make it an inevitable choice to be used in a broad-spectrum of applications such as biomedical, water and air purification, food production, cosmetics, clothing, and numerous household products. Silver in the form of metallic silver nanoparticles [1], Dendrimer–silver nanoparticle complexes and composites [2],

* Corresponding author. Tel.: +91 9444345049.
E-mail address: cynprin@gmail.com (G.C.J. Swarnavalli).
Peer review under responsibility of King Saud University.

ELSEVIER Production and hosting by Elsevier

http://dx.doi.org/10.1016/j.jscs.2015.03.004
1319-6103 

polymer silver nanoparticle composites [3] and silver nanoparticles coated onto polymers like polyurethane [4] has been currently considered for potential antibacterial activity. However there is serious concern regarding the synthetic procedure involved where toxic reducing agents, capping agents and solvents have been used. Therefore, it is desirable and almost becoming a priority to opt for alternative green synthetic method for nanomaterial synthesis with environmentally friendly reagents [5,6]. The present decade has witnessed the rapid shift in synthesis strategies from physicochemical methods to biological methods involving use of bacteria, fungi and phytochemicals for nanoparticle synthesis [7]. Employing biomaterials in nanoparticle synthesis is not something new since it is a well established fact that the various organisms such as diatoms, magnetostactic and S-layer bacteria are capable of synthesizing nanoscale materials [8]. Biomaterials as reducing/capping agent are a viable alternative to the current physicochemical methods which utilize intense energy, hazardous chemicals and are expensive. Recent literature abounds with reports showing feasibility of extracellular biological methods of synthesis of silver nanoparticles by utilizing extracts from plants and intracellular methods utilizing bio-organisms as reducing agent, capping agents or both [9]. Plant extracts from various plants such as *Capsicum annuum* L., *Pongamia pinnata* (L.) *Pierre*, Persimmon, Geranium, *Pulicaria glutinosa* and Pine leaves have been used as reducing agents to synthesize silver nanoparticles [9–14]. Bio-reduction of gold and silver ions to yield metal nanoparticles using Geranium leaf broth, Neem leaf broth, lemongrass extract, Tamarind leaf extract, Aloe vera plant extracts [15–19] was also reported.

In this work, we explore the potential use of shadow-dried pericarp of *Sapindus emarginatus* in the synthesis of silver nanoparticles (AgNPs). *S. emarginatus* is a small deciduous tree found in the hilly regions of south India and commonly known as soap nut. Pericarps of the plant were found to contain large percentage of triterpenoid saponins Kaempferol, Quercetin and β-sitosterol. The triterpenoid saponin was also isolated and characterized. The structure was elucidated as hederagenin 3-O-(2-O-acetyl-β-D-xylopyranosyl)-(1 → 3)-α-L-rhamnopyranosyl-(1 → 2)-α-L-arabinopyranoside [20]. The study also documents the antibacterial activity of the as synthesized AgNps. The silver nanoparticles were characterized by X-ray diffraction analysis (XRD), transmission electron microscopy (TEM), high resolution transmission electron microscopy (HRTEM) and FTIR and ultraviolet–visible (UV–vis) spectroscopy. The efficacy of the biologically synthesized nanoparticles as potent antibacterial agents against certain clinically significant gram negative and gram positive bacteria is discussed.

## 2. Materials and methods

Dried pericarp of *S. emarginatus* has been purchased from local Ayurvedic store and authenticated. The pericarp of dried soapberries is shown in Supplementary data Fig. S1a. Silver nitrate $AgNO_3$ (99.9%) was purchased from Qualigen chemicals. Deionized water was used in all the experiments.

### 2.1. Preparation of the S. emarginatus extract (SEE)

About 50 g of the pericarp of *S. emarginatus* was washed thoroughly with distilled water and shade dried for 5 days. The dried pericarp was crushed using mortar and pestle. The crushed material was mixed with 100 mL of deionized water in a beaker and allowed to soak overnight and kept in a thermostat at 60 °C for 30 min. The extract was filtered with Whatman filter paper No 1. The filtered SEE was golden yellow in color (Supplementary Fig. S1b) and stored in refrigerator at 4 °C for further studies. No characteristic absorption was observed in visible region for the extract. The same filtrate was used as reducing/capping agent to control and regulate the size and shape of the nanoparticles during synthesis.

### 2.2. Synthesis of silver nanoparticles

A set of three samples were synthesized and labelled as S-1, S-2 and S-3, respectively. Sample (S-1) was synthesized by treating 20 mL of silver nitrate solution (1 mM) and 10 mL of SEE. To this solution was added 2 mL of sodium hydroxide and the mixture was stirred for 20 min. The solution was then heated in a thermostat for 3 h at 35 °C when the solution turned yellowish brown indicating the formation of silver nanoparticles. A black precipitate was obtained by centrifuging the solution at 16,000 rpm. The precipitate was washed repeatedly to remove any water soluble biomolecules present. The same experiment was repeated with different heating duration, reaction temperature and extract quantity for the preparation of sample S-2 (1 h, 70 °C, 10 mL) and S-3 (1 h, 70 °C, 15 mL) respectively. The as synthesized samples are shown in Supplementary Fig. S2.

### 2.3. Characterization of silver nanoparticles

Powder X-ray diffraction (PXRD) analysis was performed using RICHSEIFER powder diffractometer, using nickel filtered copper K-alpha radiations ($\lambda$ = 1.5461 Å) with a scanning rate of 0.02°. FTIR spectra were recorded for the solid samples in a Perkin Elmer Spectrum ES version. UV–visible spectra of the silver sols were recorded using a Cary 5E UV–VIS–NIR Spectrophotometer. TEM and HRTEM images of the silver nanoparticles were recorded using a JEOL JEM 3010 instrument with a UHR pole piece electron microscope operating at 200 kV.

### 2.4. Antibacterial studies

The antibacterial activity of silver nanoparticles was studied against the pure cultures of *Bacillus subtilis* (MTCC 441), *Staphylococcus aureus* (MTCC 96), *Escherichia coli* (MTCC 443), *Proteus mirabilis* (MTCC 1429), *Proteus vulgaris*, *Klebsiella pneumonia*, *Pseudomonas aeruginosa* (MTCC 424) and *Vibrio cholerae*. The cultures were obtained from Microbial Type Culture Collection (MTCC), Chandigarh, India and were maintained on nutrient agar slants at refrigerated condition. The 18 h-revived cultures were prepared in nutrient broth (composition (g/L): peptone 5.0; yeast extract 2.0; sodium chloride 5.0) at a pH of 7 and in one liter distilled water. The Muller Hinton Broth was used for antibacterial assays (composition in (g/L) Beef extract powder 2.0 Acid digest of casein 17.5 Starch 1.5).

### 2.5. Minimal inhibitory concentration of active compounds

Minimal inhibitory concentration (MIC) determinations were performed in sterilized 96 well microtitre plates. A serial

dilution containing the growth medium and compounds was prepared to a volume of 100 μL per well. To this, a 10 μL aliquot of the test organism (adjusted to a 0.5 McFarland standard in 0.85% (w/v) saline solution) was added to each well. Positive controls were also prepared. All the dilutions and controls were prepared in triplicate. The plates were incubated under aerobic conditions for 16 h, depending on the bacterium used. After the appropriate incubation time, each well was added with 10 μL of MTT (thiazolyl blue tetrazolium bromide) at the concentration of 5 mg/mL sterile distilled water, to differentiate the live and dead cells. Finally, the microtitre plate was mixed thoroughly and the optical density was measured at 575 nm, in triplicate, using an Emax Precision Microplate Reader (Molecular Devices). The MIC was then determined at the concentration where there was no increase in the 575 nm. The experiment was repeated in triplicate to check for reproducibility.

## 3. Results and discussion

The addition of silver nitrate ($AgNO_3$) solution to the *S. emarginatus* extract, results in the solution changing color from golden yellow to yellowish brown. Addition of sodium hydroxide to the reaction mixture accelerates the formation of silver nanoparticles. Since SEE contains reducing sugars alkaline medium favors reduction [21]. The observed color changes are due to surface plasmon vibrations of silver nanoparticles. Fig. 1 shows optical absorption spectra of SEE and three samples (S-1, S-2 and S-3). The absorption spectrum of SEE extract is transparent in the entire visible region and a peak is observed at 268 nm, which is due to $\pi$–$\pi^*$ and n–$\pi^*$ transitions and this indicates the presence of —OH and/or —C═O groups in SEE [22]. The synthesized silver samples show Surface Plasmon Resonance (SPR) peaks at 418, 413 and 415 nm for S-1, S-2 and S-3 respectively along with the SEE extract peak at 268 nm. SPR band in this region strongly suggests the formation of spherical silver nanoparticles [23]. The extract peak observed in the synthesized samples indicates the presence of extract as capping agent. Sharp peak observed for S-1 indicates that the nanoparticles are of uniform size. Broad absorption spectrum of S-2 and S-3 depicted the distribution of different size silver nano particles. The observed very small blue shift in $\lambda_{max}$ indicates reduction in size of the particles.

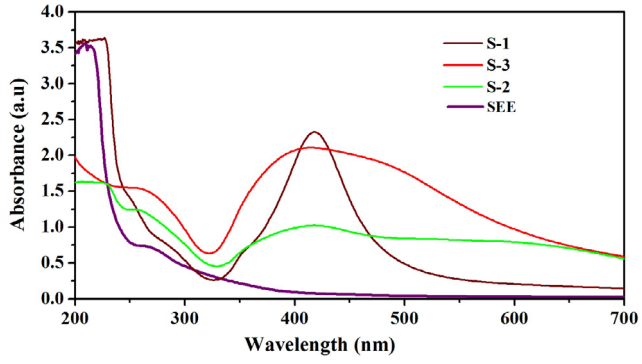


**Figure 1** UV–vis absorption spectra of SEE and AgNPs (S-1, S-2 and S-3).

TEM images show quite uniform sized silver nanoparticles that are formed by reduction of $Ag^+$ ions with the extract of the pericarp of *S. emarginatus*. The particles are predominantly spherical with smooth surfaces as shown in Fig. 2(a)–(f). Low magnification TEM images of samples S1, S-2 and S-3 show large number of silver nanoparticles which are moderately mono dispersed with size ranging from 5 to 20 nm (Fig. 2a–c). HRTEM image of all the three samples (Fig. 2d–f) shows clear spherical morphology of silver nanoparticles. Particle size distribution plots for the three samples are shown in Fig. 3(a)–(c). The average particle size of the nanoparticles in samples S-1, S-2 and S-3 is 10, 8 and 6 nm, respectively. These nanoparticles appear to have assembled into very open, quasi-linear superstructures rather than a dense closely packed assembly [15]. The figure also reveals that nanoparticles are not in contact but are evenly separated.

X-ray diffraction analysis was carried out to confirm the crystalline nature of the silver nanoparticles. The XRD patterns of the annealed silver nanoparticles are shown in Fig. 4. The observed results are in good agreement with the JCPDS Card No. 65-2871. XRD spectra show a peak at 38.20°, 44.23° and 64.33° which corresponds to (1 1 1), (2 0 0) and (2 2 0) planes of face-centred cubic (FCC) crystalline silver nanoparticles. This confirms the formation of face-centred cubic (FCC) crystalline silver nanoparticles by the reduction of $Ag^+$ ions by the SEE.

FTIR spectra of lyophilized sample of *S. Emarginatus* pericarp extract and freshly prepared AgNps-SEE are given in Fig. 5a and b. The FTIR spectrum of the SEE shows the presence of alcoholic —OH (3412 $cm^{-1}$, broad) that is due to the presence of natural flavanols, which is further confirmed by the presence of an intense peak at 1050 $cm^{-1}$ due to C—$O_{str}$ in alcohols. Broadband at 3412 $cm^{-1}$ indicates its glycosidic nature. The intense bands at 2931 and 2855 $cm^{-1}$ indicate the presence of aliphatic —C—$H_{str}$. Presence of the carbonyl group is confirmed by intense bands at 1730 and 1693 $cm^{-1}$. Methyl groups are also present (1453 and 1383 $cm^{-1}$ peaks, —CH—$_{def}$ bands of —$CH_3$). Presence of some weak aromatic —CH peaks have also been observed (920–780 $cm^{-1}$). The freshly prepared silver nanoparticles also show all the typical absorption bands present in the SEE indicating the role of metabolites present in the pericarp of *S. Emarginatus* as capping agent.

Extracts of various plants have been successfully used in the synthesis of noble metal nanoparticles where the size of the particle is generally greater than 20 nm. The present work demonstrated that discrete nanoparticles of size $<20$ nm were synthesized in the presence of extract of pericarp of *S. emarginatus*. A comparison with the literature is given in Table 1. The facile manner in which the reduction of $Ag^+$ and capping of the silver nanoparticles is accomplished by the use of the SEE is not surprising because Hederagenin, the triterpenoid saponin present in the pericarp on hydrolysis yields three reducing sugars. The sugars are namely D-glucose, D-xylose, and L-rhamnose that may actively take part in the reduction of $Ag^+$ to metallic silver. The triterpene-glycosides present in the pericarp are amphipolar under certain conditions and thus can act as a capping agent which accounts for the monodispersity, non agglomeration and stability of the silver nanoparticles. Moreover it was observed that the three samples prepared under conditions of different temperature

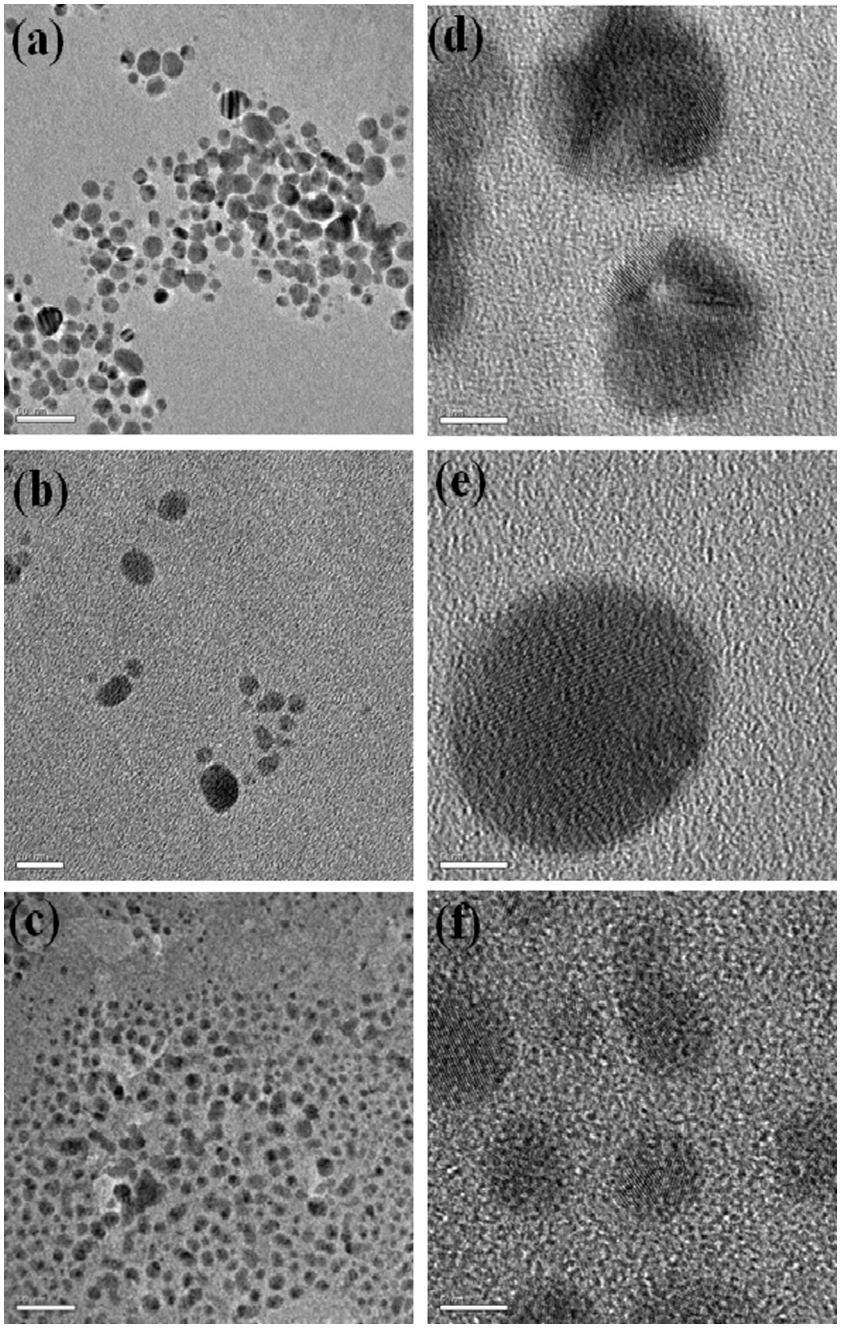


**Figure 2** TEM images of AgNPs (a) S-1 (Scale bar 50 nm), (b) S-2 (Scale bar 20 nm), (c) S-3 (Scale bar 50 nm) and HRTEM image of AgNPs (d) S-1 (scale bar 5 nm), (e) S-2 (scale bar 5 nm), (f) S-3 (scale bar 5 nm).

(room temperature, 70 °C) and amount of SEE (10 mL, 15 mL) have similar morphology with small variation in particle size. This shows that this is a facile, green and cost effective method of synthesis for silver nanoparticles.

The antibacterial activity of sample S-1 (which was one month old and contained spherical silver nanoparticles of average size 10 nm) was assessed against commonly prevalent clinically significant bacterial strains; Gram positive bacteria – *B. subtilis*, *S. aureus* and other gram negative bacteria like *E. coli*, *P. mirabilis*, *K. pneumonia*, *P. aeruginosa* and *Vibrio cholerae*, respectively. The results indicate a near 100% inhibition of the majority study microorganisms at a concentration range of 31.25 μg/mL onwards (Fig. 6). In the entire spectrum of organisms tested, *P. aeruginosa* is reported to have higher susceptibility. The increase in concentration range from 0.49 to 250 μg/mL has resulted in a proportional increase in percentage of inhibition which indicates that at higher concentrations this particular sample of silver nanoparticle is more efficient as an antibacterial agent. When compared to the S-1, S-1 (new) which is a freshly prepared sample exhibits a better inhibition spectrum in that it exhibits a higher percentage of inhibition towards gram-positive bacteria namely; *B. subtilis*

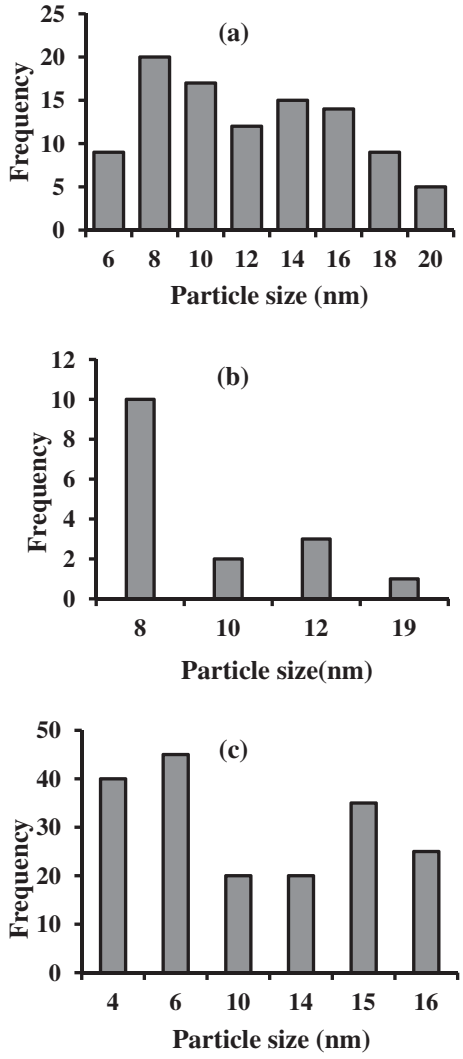


**Figure 3** Particle size distribution plots of (a) S-1, (b) S-2, (c) S-3.

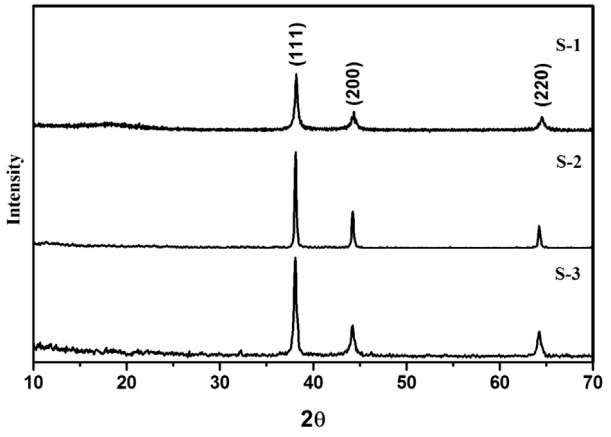


**Figure 4** Powder XRD spectra of annealed samples of AgNPs (a) S-1, (b) S-2, (c) S-3.

and methicillin-resistant *S. aureus* along with other gram-negative bacteria namely *E. coli* and *P. mirabilis* (Fig. S3-Supplementary data).

Sample S-2 (spherical silver nanoparticles of the same size as in sample S-1 with greater degree of monodispersity) is more effective against *V. cholerae*, *P. aeruginosa* and *K. pneumonia* gram-negative members of the Gammaproteobacteria (Fig. 7). This comprises several medically and scientifically important groups of bacteria, such as the Enterobacteriaceae, Vibrionaceae and Pseudomonadaceae. A number of important pathogens belong to this class, e.g. *Salmonella* spp. (enteritis and typhoid fever), *Yersinia pestis* (plague), *V. cholerae*, *P. aeruginosa* (lung infections in hospitalized or cystic fibrosis patients), and *E. coli* (food poisoning). At lower concentrations this specific nanoparticle is found to inhibit the growth of not only the members of Vibrionaceae and Pseudomonadaceae but also the Bacillus species used in the study. This sample (S-2) is found to be very effective in inhibiting *Proteus* spp. and *Pseudomonas* spp. gram negative bacterium when compared to other members of test organisms.

The freshly prepared sample S-3 (contains nanoparticles of average size 6 nm) exhibits a better inhibition spectrum in that it has higher percentage of inhibition towards gram-positive bacteria namely, *B. subtilis*; and *S. aureus* along with gram-negative bacteria (Fig. 8 and Fig. S-4-Supplementary data). This trend is similar to the one observed with S-1 nanoparticles but the overall percentage of inhibition is higher when compared to S-1 and S-2 which could be attributed to the smaller particle size in the range of 6 nm as compared to the range of 10 nm of the other nanoparticles.

It was reported in the literature that the antibacterial effect of silver nanoparticles improves with a decrease in size of the particles. As size decreases surface area to volume ratio (SA/V) for individual particle increases which results in the increase in relative particle concentration [30]. It was shown that smaller particles (size $< 10$ nm) exhibited higher efficiency which may be due to high particle penetration at smaller size [31,32].

Results are consistent with that of earlier studies. Smaller silver nanoparticles demonstrated higher efficacy as antibacterials against both pathogenic and non-pathogenic bacterial strains. This may be attributed to the maximum contact area which is a direct consequence of larger SA/V ratio. Although, the probable reason for antibacterial activity of silver nanoparticles cannot be fully explained by either release of $Ag^+$ ions or by direct contact, significant improvement in the efficacy for nanoparticles particularly below the 10 nm size range is largely attributed to the contact mode killing mechanism [30].

Structural changes in the cell membrane occur because of the ability of silver nanoparticles to anchor themselves to the bacterial cell wall. Thus the cell membrane is penetrated leading to cell death. Sondi et al. have shown that antibacterial activity of silver nanoparticles on gram negative bacteria is dependent on the concentration of silver nanoparticles [33]. The nanoparticles induce pit formation on the bacterial cell wall into which the silver nanoparticles accumulate. This causes permeability of the cell membrane and cell death. In another mechanistic view the cells may perish due to the formation of free radicals by the silver nanoparticles. There have been electron spin resonance spectroscopy studies that suggested that there is formation of free radicals by the silver nanoparticles when in contact with the bacteria, and these free radicals have the ability to damage the cell membrane and make it porous which can ultimately lead to cell death [34,35].

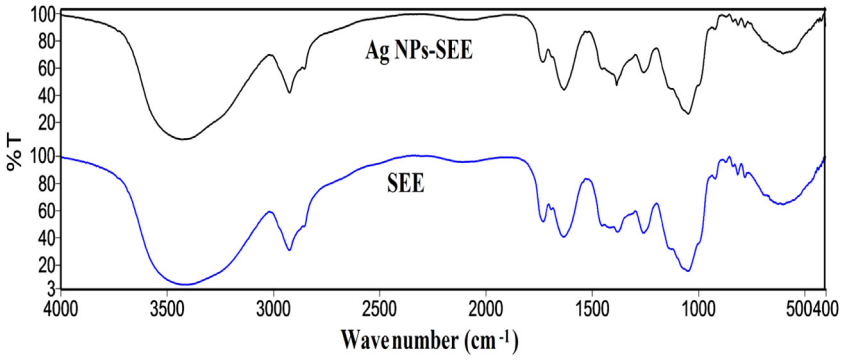


**Figure 5** FTIR spectra of *Sapindus emarginatus* pericarp extract and freshly prepared AgNps-SEE.

**Table 1** Comparison of AgNP size with different bio-reducing agents.

| Source | Types and size of NPs (nm) | References |
|---|---|---|
| *Pongamia pinnata* (L.) *Pierre* | Ag 38 aggregated non uniform size | [11] |
| *Azadirachta indica* | Ag, Au 50/100 (polydispersed) | [13] |
| *Aloe vera* | Au 50/350 | [19] |
| *Cinnamomum camphora* | Ag 50 | [24] |
| *Murraya koenigii* | Ag 40–80 | [25] |
| | 10–25 aggregated Ag | [26] |
| *Plumeria rubra* | Ag 30–200 | [27] |
| *Citrus aurantium* | Ag > 50 | [27] |
| Geranium leaf plant extract | Ag 16/40 | [15] |
| *Jatropha curcas* | Ag > 20 | [28] |
| *Tridax procumbens* | Ag > 20 | [28] |
| *Hibiscus rosasinensis* | Ag 13/20 | [29] |
| *Sapindus emarginatus* | Ag 5–20 | Present work |

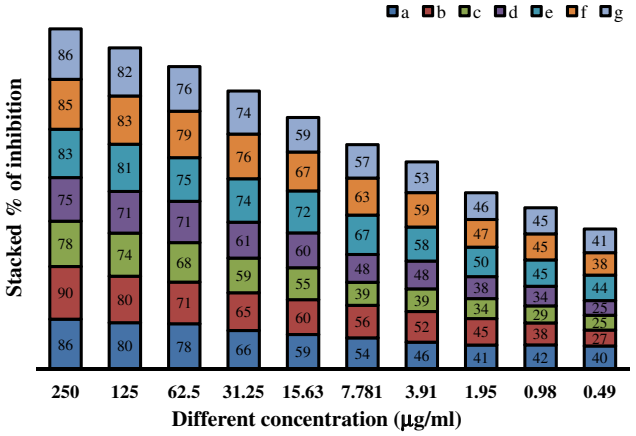


**Figure 7** S-2 Inhibition spectrum at different concentrations. (a) *Bacillus subtilis*, (b) *Staphylococcus aureus*, (c) *Escherichia coli*, (d) *Proteus mirabilis*, (e) *Klebsiella pneumonia*, (f) *Pseudomonas aeruginosa*, (g) *Vibrio cholerae*.

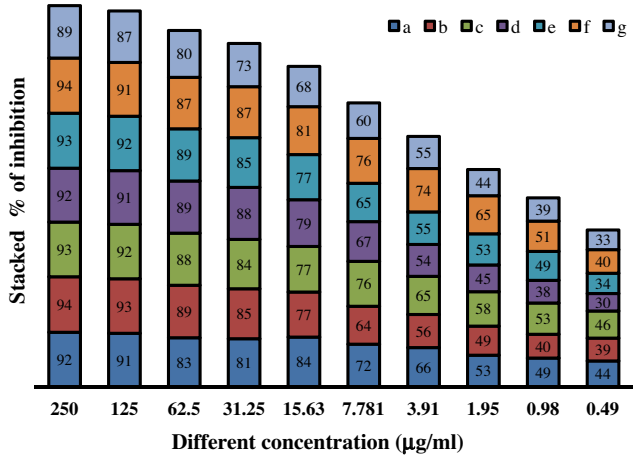


**Figure 6** S-1 Inhibition spectrum at different concentrations. (a) *Bacillus subtilis*, (b) *Staphylococcus aureus*, (c) *Escherichia coli*, (d) *Proteus mirabilis*, (e) *Klebsiella pneumonia*, (f) *Pseudomonas aeruginosa*, (g) *Vibrio cholerae*.

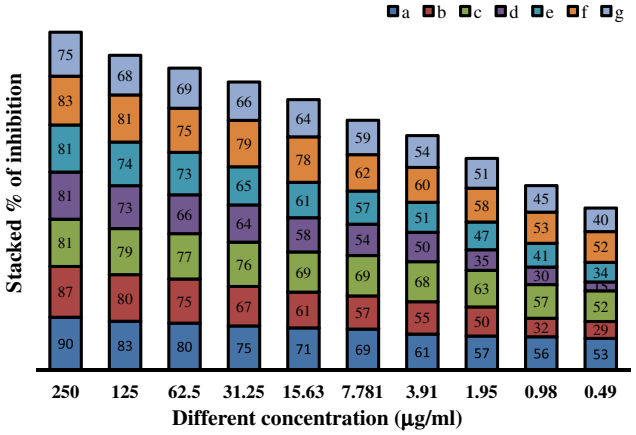


**Figure 8** S-3 (new) Inhibition spectrum at different concentrations. (a) *Bacillus subtilis*, (b) *Staphylococcus aureus*, (c) *Escherichia coli*, (d) *Proteus mirabilis*, (e) *Klebsiella pneumonia*, (f) *Pseudomonas aeruginosa*, (g) *Vibrio cholerae*.

It has been proposed that the silver nanoparticles release silver ions [36], and these ions can interact with the thiol groups of many vital enzymes and inhibit several functions in the cell and damage the cells [37]. However, to understand the complete mechanism further research is required on the topic to thoroughly ascertain the claims [38].

The present study reports significant activity of phytogenic nanoparticles against the selected pathogenic strains and the minimum amount of silver nanoparticles required was less to bring about the inhibition of the growth of the strains. The antibacterial sensitivity of the gram-positive *S. aureus* was lower than that of the gram-negative *E. coli*. This may possibly be attributed to the thickness of the peptidoglycan layer of *S. aureus*. The vital function of the peptidoglycan layer is to protect against antibacterial agents such as degradative enzymes, antibiotics, toxins and chemicals. This result agrees with the results of previous studies [36,39]. The Gram negative cell envelope consists of outer membrane, thin peptidoglycan layer, and cell membrane. Beside this, gram positive cell envelope consists of lipoteichoic acid containing thick peptidoglycan (30–100 nm) layer and cell membrane. The thick peptidoglycan layer of gram positive bacteria may protect formation of pits or ROS by Ag-nanoparticles more severely than thin peptidoglycan layer of gram negative bacteria [40]. However an interesting observation of this study is that silver nanoparticles of average size 6 nm and freshly prepared samples demonstrated enhanced activity against gram positive bacteria *B. subtilis* and *S. aureus*. This can be attributed to higher particle penetration and availability of more area of contact between the bacterial cell and nanoparticles.

## 4. Conclusion

Synthesis of spherical silver nanoparticles using shadow-dried *S. emarginatus* pericarp extract (SEE) was quite fast and nanoparticles were formed at room temperature and at 70 °C within an hour of silver ion coming in contact with the extract. This shows that this is a facile method comparable to any chemical method of synthesis for spherical silver nanoparticles of size $< 20$ nm even at room temperature. Further it is cost effective and environmentally friendly. The size of the nanoparticles achieved shows that the extract not only promotes the formation of stable spherical silver nanoparticles but it was also found to be a good capping agent. All the three samples exhibit almost similar bactericidal activity which may be attributed to the similar size and shape of the nanoparticles. The spherical silver nanoparticles were found to have wider antibacterial activity in gram negative organisms than the gram positive one. It was also observed that freshly prepared samples and smaller nanoparticles have enhanced activity against gram positive organisms *B. subtilis* and *S. aureus*.

## Acknowledgements

We sincerely acknowledge the facilities provided by Sophisticated Analytical Instruments Facility (SAIF) IIT Madras and Department of nuclear Physics, University of Madras, Guindy Campus, Chennai, India.

## Appendix A. Supplementary data

Supplementary data associated with this article can be found, in the online version, at http://dx.doi.org/10.1016/j.jscs.2015.03.004.

## References

[1] S. Arora, J. Jain, J. Rajwade, K. Paknikar, Toxicol. Lett. 179 (2008) 93.
[2] L. Balogh, D. Swanson, D. Tomalia, G. Hagnauer, A. McManus, Nano Lett. 1 (2001) 18.
[3] S. Bajpai, Y. Mohan, M. Bajpai, R. Tankhiwale, V. Thomas, J. Nanosci. Nanotechnol. 7 (2007) 2994.
[4] P. Jain, T. Pradeep, Biotechnol. Bioeng. 90 (2005) 59.
[5] P. Malik, R. Shankar, V. Malik, N. Sharma, T.K. Mukherjee, J. Nanopart. 2014 (2014) 302429.
[6] Mujeeb Khan, Merajuddin Khan, Mufsir Kuniyil, Syed Farooq Adil, Abdulrahman Al-Warthan, Hamad Z. Alkhathlan, Wolfgang Tremel, Muhammad Nawaz Tahir, Mohammed Rafiq H. Siddiqui, Dalton Trans. 43 (2014) 9026.
[7] K. Prasad, K.J. Anal, A.R. Kulkarni, Nanoscale Res. Lett. 2 (2007) 248.
[8] D. Pum, U.B. Sleytr, Trends Biotechnol. 17 (1999) 8.
[9] S. Li, Y. Shen, A. Xie, X. Yu, L. Qiu, L. Zhang, Q. Zhang, Green Chem. 9 (2007) 852.
[10] Rajesh W. Raut, Niranjan S. Kolekar, Jaya R. Lakkakula, Vijay D. Mendhulkar, Sahebrao B. Kashid, Nano-Micro Lett. 2 (2010) 106.
[11] J.Y. Song, B.S. Kim, Korean J. Chem. Eng. 25 (2008) 808.
[12] S.S. Shankar, A. Rai, A. Ahmad, M. Sastry, Appl. Nanotechnol. 1 (2004) 69.
[13] Mujeeb Khan, Shams Tabrez Khan, Merajuddin Khan, Syed Farooq Adil, Javed Musarrat, Abdulaziz A. Al-Khedhairy, Abdulrahman Al-Warthan, Mohammed Rafiq H. Siddiqui, Hamad Z. Alkhathlan, Int. J. Nanomed. 9 (2014) 3551.
[14] J. Kasthuri, S. Veerapandian, N. Rajendiran, Colloids Surf. B: Biointerfaces. 68 (2009) 55.
[15] S.S. Shankar, A. Ahmad, M. Sastry, Biotechnol. Prog. 19 (2003) 1627.
[16] S.S. Shankar, A. Rai, A. Ahmad, M. Sastry, J. Colloid Interface Sci. 275 (2004) 496.
[17] S.S. Shankar, A. Rai, A. Ahmad, M. Sastry, Chem. Mater. 17 (2005) 566.
[18] B. Ankamwar, M. Chaudhary, M. Sastry, Synth. React. Inorg. Metal-Org. Nanometal Chem. 35 (2005) 19.
[19] S.P. Chandran, M. Chaudhary, R. Pasricha, A. Ahmad, M. Sastry, Biotechnol. Prog. 22 (2006) 577.
[20] A. Sharma, S.C. Sati, O.P. Sati, D. Sati, S.K. Maneesha Kothiyal, Int. J. Res. Ayurveda Pharm. 2 (2011) 403.
[21] Majid Darroudi, Mansor Bin Ahmad, Abdul Halim Abdullah, Nor Azowa Ibrahim, Kamyar Shameli, Int. J. Mol. Sci. 11 (2010) 3898.
[22] T. Peter Amaladhas, S. Sivagami, T. Akkini Devi, N. Ananthi, S. Priya Velammal, Adv. Nat. Sci.: Nanosci. Nanotechnol. 3 (2012) 045006.
[23] G. Mie, Ann. Phys.-Berlin 25 (1908) 377.
[24] J. Huang, Q. Li, D. Sun, Y. Lu, Y. Su, X. Yang, H. Wang, Y. Wang, W. Shao, N. He, J. Hong, C. Che, Nanotechnology 18 (2007) 105104.
[25] S.R. Bonde, D.P. Rathod, A.P. Ingle, R.B. Ade, A.K. Gade, M.K. Rai, Nanosci. Methods 1 (2012) 25.
[26] L. Christensen, S. Vivekanandhan, M. Misra, A. Mohanty, Adv. Mater. Lett. 2 (2011) 429.

[27] C.D. Patil, S.V. Patil, H.P. Borase, B.K. Salunke, R.B. Salunkhe, Parasitol. Res. 110 (2012) 1815.
[28] R. Pala, U.R. Pathipati, S. Bojja, J. Nano Part. Res. 12 (2010) 1711.
[29] P. Daizy, Physica E 42 (2010) 1417.
[30] S. Agnihotri, S. Mukherji, S. Mukherji, RSC Adv. 4 (2014) 3974.
[31] A. Panacek, L. Kvítek, R. Prucek, M. Kolar, R. Vecerova, N. Pizúrova, V.K. Sharma, T. Nevecna, R. Zboril, J. Phys. Chem. B 110 (2006) 16248.
[32] J.R. Morones, J.L. Elechiguerra, A. Camacho, K. Holt, J.B. Kouri, J.T. Ramirez, M.J. Yacaman, Nanotechnology 16 (2005) 2346.
[33] I. Sondi, B. Salopek-Sondi, J. Colloid Interface Sci. 275 (2004) 177.
[34] M. Danilcauk, A. Lund, J. Saldo, H. Yamada, J. Michalik, Spectrochim. Acta A 63 (2006) 189.
[35] J.S. Kim, E. Kuk, K. Yu, J.H. Kim, S.J. Park, H.J. Lee, S.H. Kim, Y.K. Park, Y.H. Park, C.Y. Hwang, Y.K. Kim, Y.S. Lee, D.H. Jeong, M.H. Cho, Nanomed. Nanotechnol. Biol. Med. 3 (2007) 95.
[36] Q.L. Feng, J. Wu, G.Q. Chen, F.Z. Cui, T.N. Kim, J.O. Kim, J. Biomed. Mater. Res. 52 (2000) 662.
[37] Y. Matsumura, K. Yoshikata, S. Kunisaki, T. Tsuchido, Mode of bactericidal action of silver zeolite and its comparison with that of silver nitrate, Appl. Environ. Microbiol. 69 (2003) 4278.
[38] S. Shrivastava, T. Bera, A. Roy, G. Singh, P. Ramachandrarao, D. Dash, Nanotechnology 18 (2007) 225103.
[39] W.K. Jung, H.C. Koo, K.W. Kim, S. Shin, S.H. Kim, Y.H. Park, Appl. Environ. Microbiol. 74 (2008) 2171.
[40] T.J. Silhavy, D. Kahne, S. Walker, The bacterial cell envelope, Cold Spring Harb. Perspect. Biol. 2 (2010) a000414.